이학석사학위논문

Fractal dimensions of bridge bonds in directed percolation models

방향성 스미기 모형에서 다리본드의 쪽거리 차원

2015년 2월

서울대학교 대학원
물리·천문학부
최상민

Fractal dimensions of bridge bonds in directed percolation models

방향성 스미기 모형에서 다리본드의 쪽거리 차원

지도교수 강병남

이 논문을 이학석사 학위논문으로 제출함

2015년 2월

서울대학교 대학원

물리·천문학부

최상민

최상민의 이학석사 학위논문을 인준함

2014년 11월

위 원 장 _____ (인)

부위원장 _____ (인)

위 원 _____ (인)

Abstract

Fractal dimensions of bridge bonds in directed percolation models

Sangmin Choi
Department of Physics and Astronomy
The Graduate School
Seoul National University

Bond percolation is a mathematical model studying the emergence of a spanning cluster as bonds are occupied in Euclidean space without any preferred direction. Bonds are classified into two types: bridge bonds and non-bridge bonds. Bridge bonds are ones that once occupied, a spanning cluster is created in one direction of the system. When the occupation of bridge bonds is prohibited and only non-bridge bonds are occupied, the system is divided into two parts; the boundary composed of bridge bonds forms a fractal object. It has been revealed that the fractal dimension of that object is related to the continuity of the so-called explosive percolation transition. In the problem of directed percolation, however, where the bonds possess a preferred direction of flow, not much is known about these bridges. We obtain the fractal dimensions of the bridges in various dimensions and compare them to those of ordinary percolation. It will further be shown that these

bridges relate to the continuity of the phase transition in the same way those of ordinary percolation do, and outline the implications of these results.

Keywords : Percolation transition, Directed percolation, Bridge bond, Distinuous percolation transition, Fractal dimension

Student Number : 2011-20426

Contents

List of figures

List of tables

Chapter 1

Introduction

Bond percolation is an area of science that studies the emergence of a path of bonds connecting two opposite surfaces. Consider a two-dimensional square lattice: For some fraction $0 \leq p \leq 1$, we occupy p of the bonds with conducting wire, while leaving $1-p$ of them unoccupied. If the occupation fraction is below a critical threshold p_c, there will be no conducting path connecting the top layer to the bottom layer. At $p = p_c$, however, a path of conduction, or percolation, emerges. The cluster of conducting wires keeps growing as p approaches unity. Due to its simplicity and effectiveness of explaining phenomena related to random media, percolation has received spotlight for decades by scientists of diverse discipline.

Now, suppose that current can only flow in one direction in the wires. One can think of this as replacing the wires with diodes. In this case, percolation is achieved only if there exists a *directed* path of conduction connecting the top and the bottom surfaces. This is called *directed percolation*, and has diverse applications in the natural world.

Directed percolation has shown interesting connections with many seemingly unrelated fields of study. In 1983 Domany and Kinzel showed the equivalence of cellular automaton and directed percolation [1]. Pomeau conjectured in 1986 that a system showing abrupt transition from a laminar state to a chaotic state can be described in terms of directed percolation [2],

which was scrutinized by studies such as [3]. Following up these works, Rolf, Bohr, and Jensen later presented strong evidence that the link between spatiotemporal intermittency and directed percolation exists only when the updating rules are asynchronous [4]. In 1998, Lopez and Jensen have shown that a model used to explain the growth of fungi colonies can be mapped onto a directed percolation process [5].

A closely related model is the directed percolation depinning(DPD) model. It studies the growth of driven interface in disordered media, and was first proposed simultaneously in 1992 by Tang et al [6] and Buldyrev et al [7]. DPD can be described by the Kadar-Parisi-Zhang equation [8] with quenched disorder [9], although it has been shown that their mechanisms of surface growth differ [10].

In the last few years, studies have been done on the boundary formed by bridge bonds, the bonds that achieve percolation upon occupation, of ordinary percolation. When the lattice is grown to its maximum capacity without connecting any bridge bonds, the system becomes partitioned into two opposing clusters, forming a boundary in between. This line, called bridge line, has been shown to have connections to concepts in different areas of study, such as optimal path cracks and watersheds [11]. Moreover, the bridge line forms a fractal structure with fractal dimension contingent on the lattice structure and the boundary conditions [12]. In a more recent study, it has been found that this fractal dimension bears direct relationship to the continuity of the percolation phase transition when the model is modified to suppress percolation rather than inhibit it [13].

In this paper, we extend the concept of fractal dimensions and their

relationship with the phase transition to the models of directed percolation. Directed percolation, with its preferred direction of flow, would behave as a more natural model to explain systems with an inclined tendency towards certain directions, an intuitive example being a watershed lying on an inclined plane such as the side of a mountain. Three types of lattice structures are considered. First, we tackle the directed square lattice, the simplest lattice in terms of both analysis and calculation. Next, we proceed to the directed body-centered cubic lattice, which is structurally equivalent to directed square lattice in $2D$. It deviates from the square lattice in three and higher dimensions, with exponentially increasing number of nearest neighbors. Then we return to the square lattice, but this time allowing directed edges only in the principal direction of percolation (vertical direction). In this lattice, all edges perpendicular to the principal direction are bidirectional. After we are done exploring the scaling behaviors of bridge bonds in thse lattices, we wrap up the study with a brief assessment of the surface roughness formed by the bridge bonds in directed percolation models.

Chapter 2

Bridge Bonds in Directed Percolation

2.1 Directed Square Lattice

Bridge bond is a bond that, once occupied, leads to the emergence of a percolating pathway between two boundary surfaces. When sequentially choosing and occupying random links, by prohibiting the occupation of bridge bonds one can artificially grow the occupation fraction p close to any desired value.

Consider a square lattice with directed bonds. Parallel bonds are set to face the same direction, thus there are d bond directions in a d-dimensional lattice. One arbitrary direction has been chosen so that percolation is defined as a directed pathway formed by a sequence of occupied bonds connecting a node at the bottom of this axis to one at its top.

Fig. 2.1 shows an example of a 100×100 2D directed lattice grown to $p \approx 1$. The color of each node indicate the boundary surface it is connected to. Unlike the case of bidirectional lattices, a bond connecting two differently colored nodes can be occupied without leading to percolation. Also, notice that each node has a preferred boundary surface. For example, in Fig. 2.1, it is more probable for a node in the upper left corner to be connected to the top surface, because the number of such possible paths outnumber that of paths connecting it to the bottom surface. A node in the lower

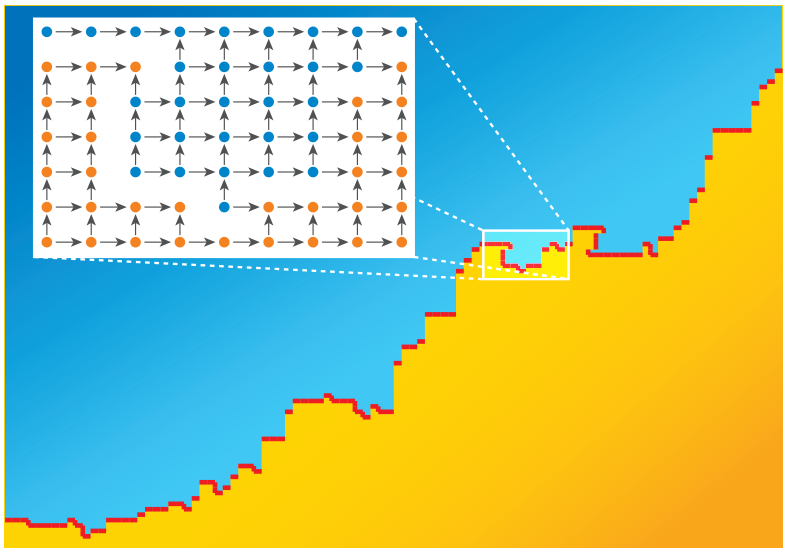

Fig. 2.1: A snapshot of a 100×100 2D lattice with directed edges at $p = 1$. Blue and yellow areas represent nodes connected to top and bottom boundaries, respectively. Solid lines indicate the locations of bridge bonds that have been suppressed in the growth. Notice the approximate 45° inclination of the boundary. The inset illustrates a magnified view of the boundary. As visible from the inset, the formulation of penninsula-like structures are possible due to the directions of the bonds.

right corner, on the other hand, will prefer the bottom surface. This discrepancy of the number of possible paths implies that the boundary formed between the two clusters will have a certain inclination, which will be more conspicuous as the size of lattice becomes larger. This is clearly shown in Fig. 2.1, with the boundary having an approximate slope of 1. The slope will be taken into account later when we calculate the roughness exponents of these boundaries.

It has been shown in [12] that in a 2D bidirectional lattice, the number of bridge bonds N_{BB} scales as $L^{1/\nu}$ at $p = p_c = 0.5$ and as $L^{1.215}$ at $p > p_c$, where d_{BB} is called the fractal dimension of the bridge bonds. We set up an *ansatz* similar to that used in [12]:

$$N_{BB} = L^{1/\nu_\parallel} F\left[(p - p_c)L^{\theta}\right], \tag{2.1}$$

where $F[x] \sim x^{\zeta}$ for $x > 0$ and $F[x] \sim$ const. for $x = 0$. $\nu_\parallel = 1.733847(6)$ and $p_c = 0.64470015(5)$ are well-established values for 2D directed bond percolation [14, 15]. Asserting that $N_{BB} \sim L^{d_{BB}}$ at p well above p_c, the following scaling relation will hold,

$$\theta = \zeta^{-1}\left(d_{BB} - \frac{1}{\nu_\parallel}\right) = \zeta^{-1}\left(d - \varphi - \frac{1}{\nu_\parallel}\right), \tag{2.2}$$

with $\varphi \equiv d - d_{BB}$.

Fig. 2.2 shows simulation results for N_{BB} in various system sizes. The number of bridge bonds at p_c and $p = 1$ clearly follow power laws with different exponents. The exponent at $p = p_c$ is measured to be 0.576, which is

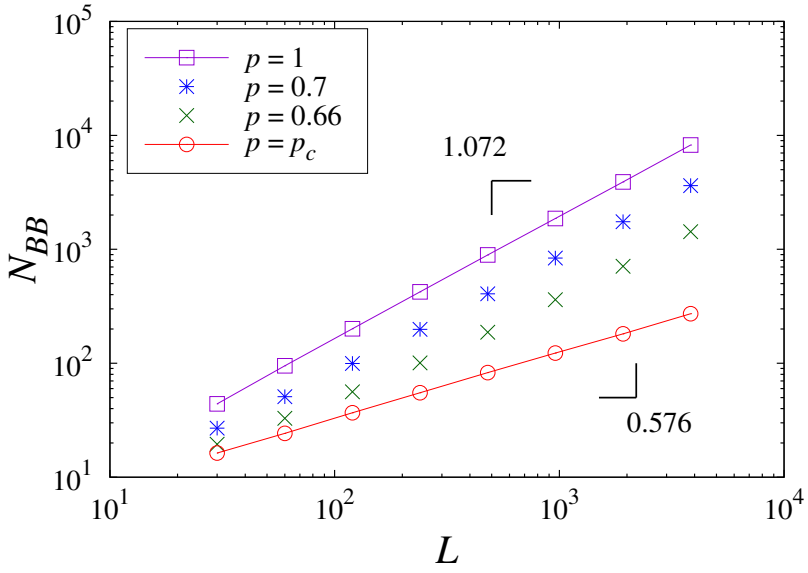

Fig. 2.2: A plot of the number of bridge bonds N_{BB} versus the linear size L in 2D directed lattice. Data points represent simulation results each averaged over 10^4 samples. At $p = p_c \approx 0.6447$ the scaling exponent is $1/\nu_{\|} \approx 0.576$, whereas at $p = 1$, $N_{BB} \sim L^{d_{BB}}$ with $d_{BB} = 1.072$. A crossover behavior can be observed as p departs from p_c.

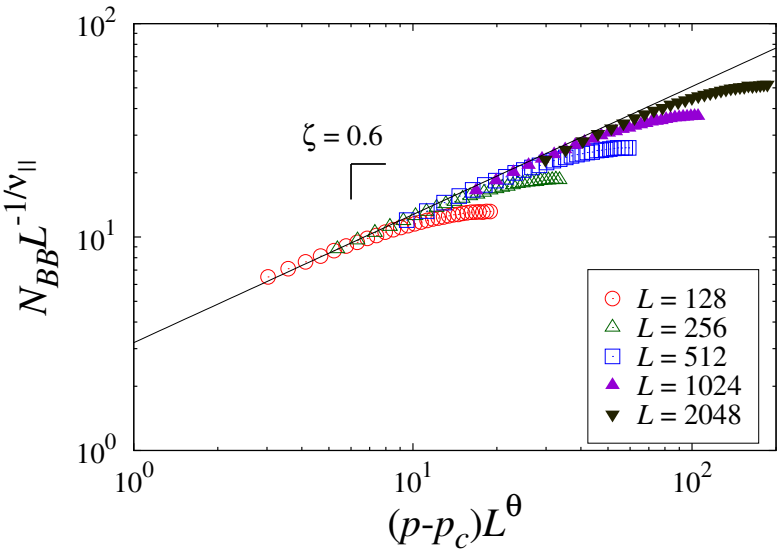

Fig. 2.3: The number of bridge bonds N_{BB} versus the occupation fraction p for 2D directed lattices. Each data point represent simulation results averaged over 10^4 samples. Both N_{BB} and p have been rescaled according to the scaling ansatz in order to obtain the growth exponent ζ, with the crossover exponent $\theta = 0.825$. From the slope of the solid line, $\zeta = 0.6$.

in excellent agreement with $1/\nu_{||} \approx 0.577$. We also obtain the fractal dimension of bridge bonds $d_{BB} = 1.072$. As expected, a crossover behavior similar to that of ordinary percolation is observed as p departs from p_c.

In order to calculate the growth exponent ζ and the crossover exponent θ, N_{BB} and p were scaled in accordance with Eq. (2.1). In Fig. 2.3 the results are plotted for various system sizes. One observes the data collapsing at $\zeta = 0.6$, along with $\theta = 0.825$.

It has recently been shown with ordinary percolation that the growth exponent ζ and the fractal dimension of bridge bonds d_{BB} are intimately related with the continuity of percolation phase transition [13]. Consider a

model in which the occupation of bridge bonds are not merely prohibited, but instead m candidates are chosen at each time step among the set of bonds that are not connected. Only in the case where all m candidates qualify as bridge bonds does one get accepted, in which case a percolating pathway emerges; otherwise a non-bridge bond is connected. In this model, the percolating threshold $p_{cm}(L)$ is a function of both m and L. The probability $q(p)$ of choosing all m candidadates to be bridge bonds at an occupation fraction p is

$$q(p) = \left[\frac{N_{BB}}{N_b(1-p)}\right]^m, \tag{2.3}$$

where N_b is the number of bonds in a fully connected square lattice. Since $N_b \sim dN^d$ and $N_{BB} \sim L^{d_{BB}}(p-p_c)^\zeta$ at $p > p_c$,

$$q(p) \sim N^{-m/m_c}\left[\frac{(p-p_c)^\zeta}{(1-p)}\right]^m \tag{2.4}$$

where m_c, the critical number of candidates, is defined to be

$$m_c = \frac{d}{d-d_{BB}}. \tag{2.5}$$

It has further been shown that for $m < m_c$, $p_{cm}(L) - p_c \sim L^{-1/\bar{\nu}_<}$ with

$$\frac{1}{\bar{\nu}_<} \equiv \frac{1}{m\zeta+1}\left(1-\frac{m}{m_c}\right), \tag{2.6}$$

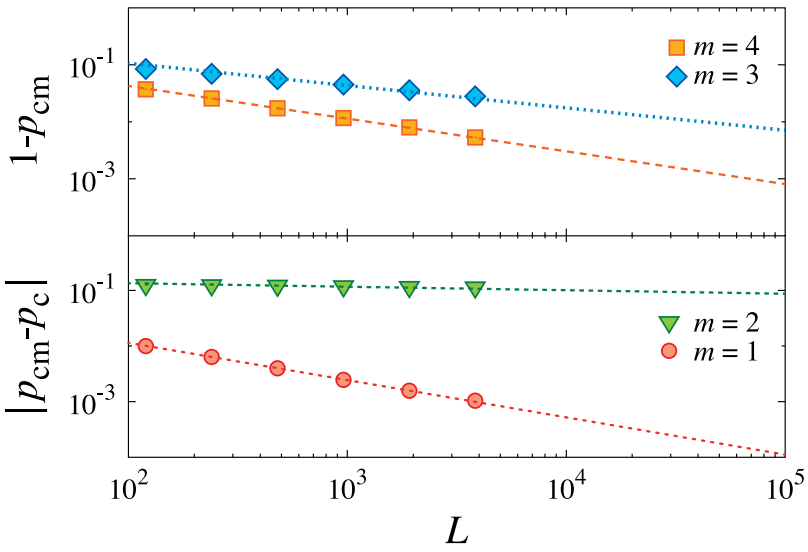

Fig. 2.4: The differences between the critical thresholds and their respective converging points are plotted against linear system size L for various m. Each data point represent simulation results averaged over 10^4 samples, and dotted lines indicate the anaylitically predicted slopes.

while for $m > m_c$, $1 - p_c \sim L^{-1/\bar{\nu}_>}$ with

$$\frac{1}{\bar{\nu}_>} \equiv \frac{1}{m-1}\left(\frac{m}{m_c} - 1\right). \tag{2.7}$$

When m is chosen to be smaller than the critical value m_c, the threshold $p_{cm}(L)$ approaches the value $p_c = 0.6447$ with increasing system size, which implies that at the thermodynamic limit $L \to \infty$ the system exhibits continuous phase transition. In contrast, if m is chosen to be larger than m_c, with growing L the threshold $p_{cm}(L)$ converges to unity; this system exhibits trivial discontinuous phase transition in the thermodynamic limit.

Since these arguments are made out of purely probabilistic reasonings

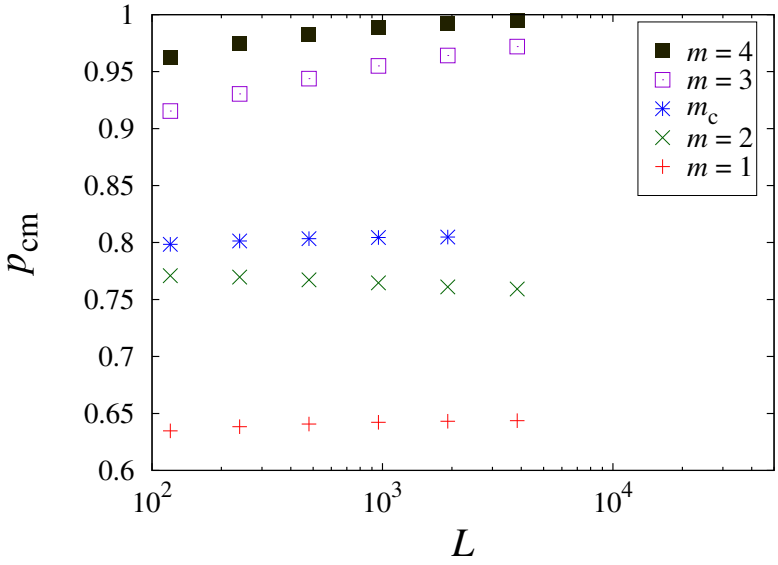

Fig. 2.5: The percolation threshold $p_{cm}(L)$ plotted against linear size L for various number of candidates m. Below m_c the thresholds converge to $p_c(\infty) = 0.6447$, whereas above m_c they converge to unity. The threshold at m_c defines a horizontal line, the phase transition above and below which are of first and of second order, respectively. Each data point represents simulation result averaged over 10^4 samples.

without any role played by the bidirectionality of bonds, we expect them to also hold in directed square lattices. Fig. 2.4 shows a plot of the simulation results in 2D directed lattices. The data points are in good agreement with the analytic expectations, which are drawn as lines. Fig. 2.5 plots p_{cm} against L for various m. As expected, the threshold at m_c draws a horizontal line above which the phase transition is discontinuous and below which it is continuous.

In bidirectional square lattices, as d increases past its upper critical dimension $d_c = 6$, the fractal dimension d_{BB} has been shown to converge to d, i.e., φ converges to 0 [12]. This implies that m_c diverges to ∞ when $d \geq d_c$, and hence the percolation phase transition in the thermodynamic limit is always continuous in this region no matter how high one chooses for m to be.

To see if this is the case for directed square lattices, d_{BB} has been measured up to $d = 6$, which is higher than the upper critical dimension $d_c = 5$ of directed percolation. Fig. 2.6 shows the results obtained, accompanied by an inset plotting the respective values of $\varphi = d - d_{BB}$. Surprisingly, φ does not come anywhere near 0, even past d_c. Therefore, unlike the case of bidirectional lattices, the phase transition of percolation in high-dimensional directed lattices can be discontinuous, by choosing $m > m_c(d)$. Fig. 2.7 iillustrates this result. The data points mark the critical values $m_c(d)$ for each d, and these form a partition curve that divides the region of first-order phase transition and that of second-order phase transition. The roman numerals indicate the order of phase transition arising in the region. Although m_c tends to increase with increasing d, no divergence to ∞ is observed.

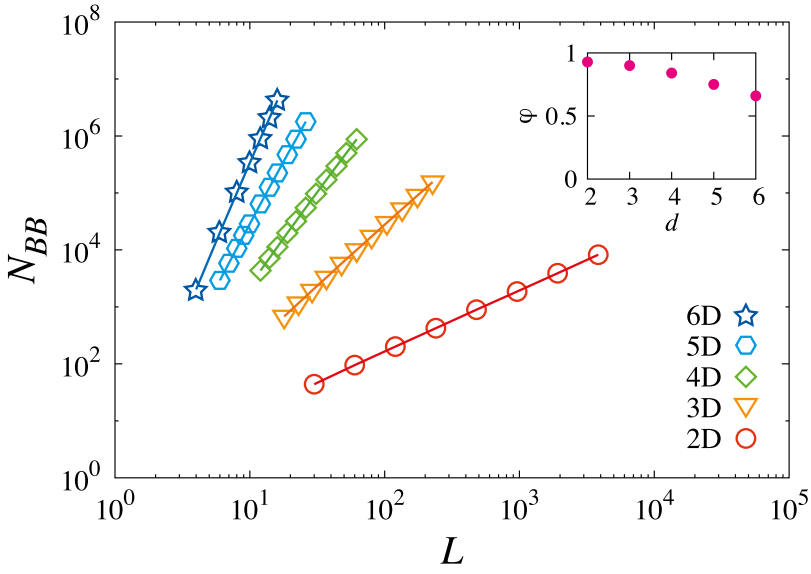

Fig. 2.6: Number of bridge bonds N_{BB} plotted against linear size L. Data points represent simulation results and solid lines represent best fits. All results have been averaged over 10^4 samples. The inset plots $\varphi = d - d_{BB}$ against d. Notice that d_{BB} stays far from d even past the upper critical dimension $d_c = 5$ of directed percolation. This indicates the presence of continuous phase transition at and above d_c.

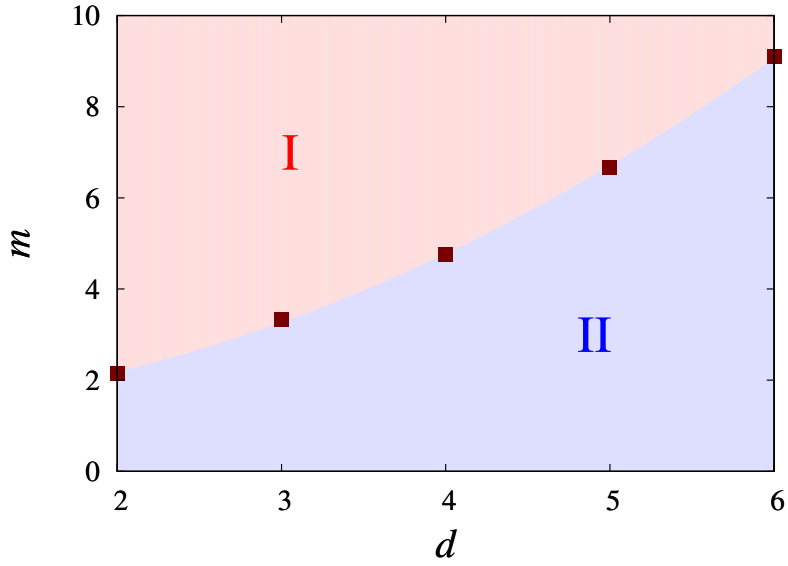

Fig. 2.7: The critical number of candidates m_c plotted for each dimension. These points form a partition curve, above which the percolation phase transition is discontinuous and below which it is continuous. Since m_c is finite even above $d_c = 5$, first-order transitions still reside in the high-m region in higher dimensions.

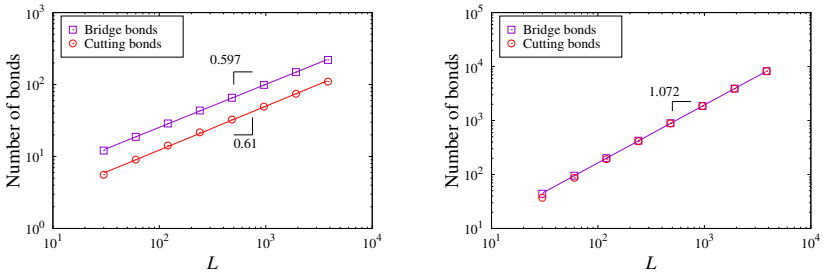

(a) At the critical point (b) At $p = 1$

Fig. 2.8: Scaling behavior of the bridge bonds and the cutting bonds. The number of bonds in (a) are measured at the point of emergence of a percolating cluster, while those in (b) are measured at a fully grown lattice excluding bridge bonds. Besides some negligible finite size effects, the number of cutting bonds coincide with that of the bridge bonds in a fully grown lattice.

Now let us consider a different type of bonds. Recall that, due to the directionality of the bonds, there can exist bonds that connect two clusters, one connected to the top and the other connected to the bottom, which does not beget percolation. How do these bonds, the cutting bonds, scale with system size?

Due to the symmetry of our directed square lattice, we expect the number of cutting bonds to be similar to the number of bridge bonds at $p = 1$. This is exactly what is observed in Fig. 2.8(b). Except for the finite size effects apparent in small-sized systems, the number of cutting bonds and that of the bridge bonds are observed to coincide for all sizes. The case at the critical point is non-trivial, however. The number of bonds at the critical points are at the point of emergence of a percolating cluster. The two types of bonds appear to scale similarly, but the bridge bonds outnumber cutting bonds with a constant factor.

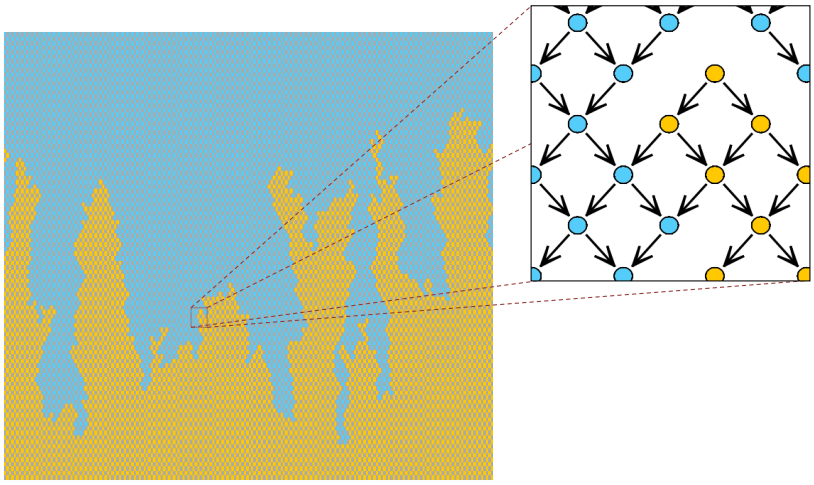

Fig. 2.9: A snapshot of a 100×100 2D tilted lattice with directed edges at $p = 1$. Blue and yellow areas represent nodes connected to top and bottom boundaries, respectively. The inset is a magnified view of a part of the boundary.

2.2 Directed Body-Centered Cubic Lattice

This time, we consider the directed body-centered cubic(BCC) lattices. In a d-dimensional directed BCC, we have L layers of $d-1$-dimensional hypercubic lattice, with each vertex having 2^d edges both incoming and outgoing. For $2D$, the structure of this lattice is equivalent to that of the directed square lattice, tilted by 45°. Taking into account the horizontal symmetry of the lattice, we impose periodic boundary consitions at the boundaries that do not determine percolation. Again, we start from an empty lattice and fill the lattice by subsequently occupying random bonds. The lattice can be grown to any desired fraction of occupation p by forbidding the occupation of bridge bonds.

L	$p_c(L)$
30	0.522735
60	0.557689
120	0.583580
240	0.601748
480	0.614410
960	0.623559
1920	0.629973
3840	0.634444

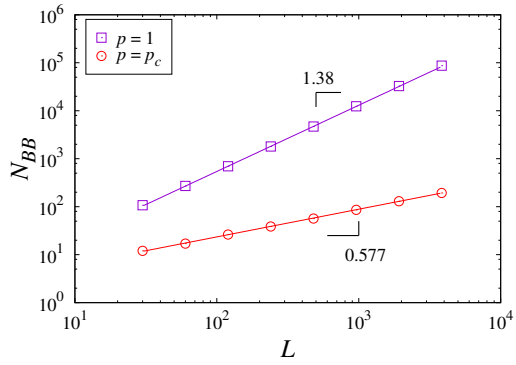

Fig. 2.10: (Left) The values of p_c measured for various system sizes in a $2D$ directed BCC lattice. Each value is an average of 10^4 independent measurements. (Right) The number of bridge bonds N_{BB} is plotted against the linear size L for 2D tilted lattice with directed edges. Each data point marks simulation results averaged over 10^4 samples. At $p = 1$, $N_{BB} \sim L^{d_{BB}}$ with $d_{BB} = 1.41$. At $p = p_c$, the scaling behavior of the bridge bonds is very similar to that of the case of square lattices. For each system size the relevant value of $p_c(L)$ was used.

Fig. 2.9 shows a sample of the directed BCC lattice grown to $p = 1$. In contrast to the case of directed square lattice, the boundary is very irregular and does not show a trend to incline in any direction, even though the structure of this lattice is nearly equivalent to the square lattice. Notice the seaweed-like structures formed at the boundary. The emergence of these structures owe to the fact that the number of possible horizontal boundaries are almost negligible to the number of boundaries of this type due to the directionality of the bonds pointing diagonally downwards.

How do the bridge bonds in this lattice scale? We again impose the *ansatz*

$$N_{BB} = L^{1/\nu_\parallel} F\left[(p - p_c)L^{\theta}\right], \tag{2.8}$$

to the number of bridge bonds N_{BB}. Observing that in $2D$ the lattice structure is equivalent to the directed square lattice, we expect N_{BB} to scale as $\sim L^{1/\nu_{||}}$ at p_c, with $\nu_{||} \approx 0.5768$. There is, however, a technical difficulty that needs consideration. For this type of $2D$ lattice, the convergence of $p_c(L)$ to the value $p_c(\infty) \approx 0.6447$ is too slow; the calculated values of $p_c(L)$ are shown on the left table of Fig. 2.10, each averaged over 10^4 samples. To more accurately measure the critical exponent, we used for each system size the appropriate value of $p_c(L)$. The results are plotted on the right of Fig. 2.10 At $p = p_c$ the exponent is measured to be ≈ 0.577, in an excellent agreement with the expected value $1/\nu_{||} \approx 0.5768$. At $p = 1$, the fractal dimension is measured to be $d_{BB} \approx 1.38$, radically different from the fractal dimensions of both the directed square lattice and the isotropic square lattice.

In order to study the percolation phase transitions in higher dimensions, we now take a look at the fractal dimensions of bridge bonds for higher-dimensional BCC lattices. Fig. 2.11 shows the results of the measurements, from which one can see that the fractal dimensions d_{BB} of bridge bonds clearly follow power law as expected. Values of d_{BB} can be read off from the inset, which plots the values of $\varphi \equiv d - d_{BB}$. Notice that φ seems to be plunging to 0 until $d = 4$, but starts to increase at and over the upper critical dimension $d_c = 5$ of directed percolation. What this indicates is that d_{BB} does not converge to d, even for $d \geq d_c$, and therefore first-order phase transition still resides above the upper critial dimension in the high-m regions. This is illustrated in Fig. 2.12, which shows the phase diagram constructed from the measurements, with roman numerals identifying the order of phase transition.

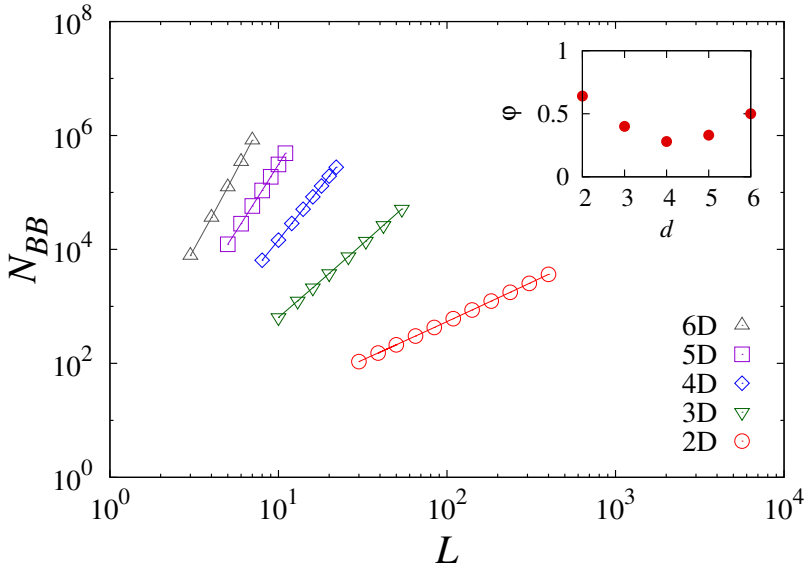

Fig. 2.11: The number of bridge bonds N_{BB} against the linear system size L for the body-centered lattice in various dimensions. Each data point represents simulation results averaged over 10^4 samples, and each solid line represents the best fit. d_{BB} becomes large for higher dimensions, but stays finite over $d > d_c = 5$.

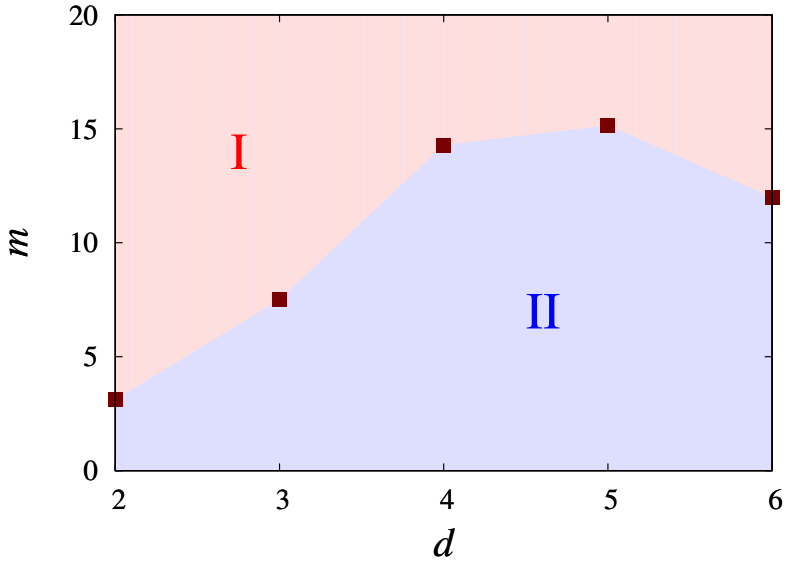

Fig. 2.12: Phase diagram constructed using the different values of $m_c(d)$ in the directed BCC lattice. Again m_c is finite above $d_c = 5$, so first-order transitions are observable in the high-m region for higher dimensions.

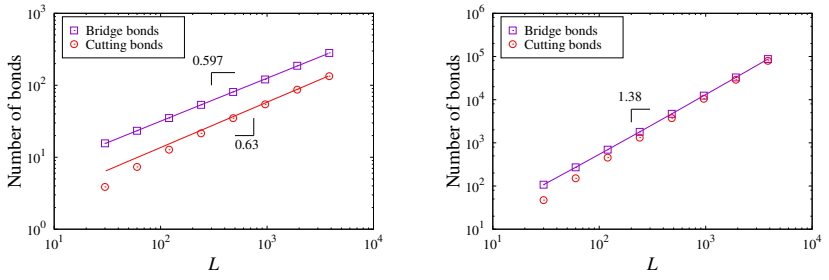

(a) At the critical point (b) At $p = 1$

Fig. 2.13: Scaling behavior of the bridge bonds and the cutting bonds for 2D tilted lattice. Again, values of (a) are measured at the point of percolation, while those in (b) are measured at $p = 1$. For this 2D lattice, finite size effect plays a larger role, but at $p = 1$ the number cutting bonds still converge to the number of bridge bonds for large L.

We now turn our attention to the cutting bonds. As was the case of directed square lattices, we measured in $2D$ the number of bridge bonds as well as the number of cutting bonds both at the point of percolation and at $p = 1$ in various system sizes. The results are plotted in Fig. 2.13. On the left, values are plotted at the critical point. On the right, at $p = 1$. The utmost difference between this lattice and the $2D$ directed square lattice is the finite size effect on the cutting bonds, which was also conspicuous for the values of p_c in Fig. 2.10. This drives the number of cutting bonds away from power law in systems of small sizes. However, one can still measure the asymptotic trends, as done in Fig. 2.13. It is shown that although the scaling exponents of the cutting bonds and the bridge bonds differ by a small amount at the critical point, it is observed that the number of cutting bonds asymptotically converge to N_{BB} at $p = 1$.

2.3 Partially Directed Square Lattice

The bonds in the directed square lattice each had a preferred direction of flow, with the restriction that parallel bonds prefer the same direction with one another. This time, consider a slightly different model, in which there is only one direction of flow instread of d. Recall that one axis was chosen so that percolation is defined as the emergence of a pathway between the two boundaries that are perpendicular to this axis. The preferred direction is aligned to be parallel to this axis. Since the subspace formed by bidirectional axes is now isotropic, we impose periodic boundary conditions along these directions.

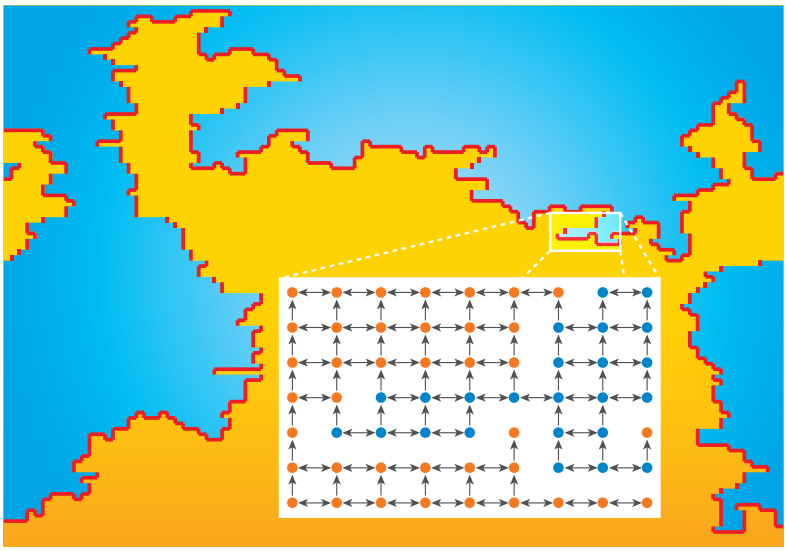

Fig. 2.14: A snapshot of a 100×100 partially directed lattice in 2D at $p = 1$. Horizontal bonds are bidirectional, whereas vertical bonds are directed upward. Blue and yellow areas represent nodes connected to the top and bottom boundaries, respectively. Solid lines indicate bridge bonds, which have been kept unoccupied to suppress percolation. Boundaries with respect to bidirectional bonds, in this case the left and right boundaries, are set to be periodic. The inset shows a magnified view of a portion of the boundary.

In this model, there is only one directional axis; the other $d-1$ axes bear bidirectional bonds. For the sake of brevity, we will henceforth call this type of system as *partially directed*. This model can be viewed as a upright square lattice imitating the properties of a tilted square lattice, in which all the bonds are directed, but the two percolation boundaries are aligned in a way to effectively render the directions parallel to them bidirectional. Fig. 2.14 is a sample of 100×100 partially directed lattice, grown to $p = 1$ excluding brige bonds on the way. Notice that the horizontal bonds are bidirectional and the left and right boundaries are therefore periodic.

One might naively expect the boundary formed by the red and blue clusters to become smooth as L increases. However, Fig. 2.14 overtly shows that this is not the case. The boundary is bizarre, far from being straight. The reason that this type of boundary is formed is because the one axis bearing a preferred direction tips the balance between pathways. In a totally bidirectional lattice, there are many chains of bonds connecting two horizontally parted nodes. In this type of lattice, however, the only pathway is a chain comprising only horizontal bonds, thereby rendering the emergence probability of such pathway very low. As we shall we in the next section, this discrepancy leads to non-trivial boundaries even for high L.

The behavior of bridge bonds in partially directed percolation has been measured. Fig. 2.15 plots the simulation results of N_{BB} against L. The fractal dimension d_{BB} in 2D is ≈ 1.4, slightly higher than that of directed lattice. This results in $m_c(d=2) \approx 3.3$, but nevertheless, as Fig. 2.16 shows, values of m smaller then m_c lead to second-order phase transition, while values higher than m_c lead to first-order. Again the values at m_c draws the dividing

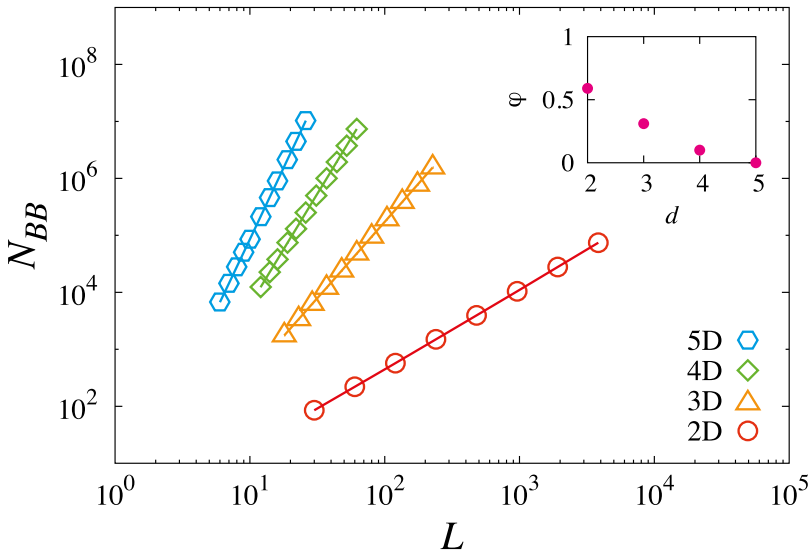

Fig. 2.15: The number of bridge bonds N_{BB} versus the linear size L in partially directed lattices. Each data points show simulation results averaged over 10^4 samples. Solid lines represent the best fits. The inset plots $\varphi = d - d_{BB}$ against d, which shows $\varphi \to 0$ as $d \to d_c = 5$. This implies that above the upper critical dimension d_c, the phase transition is always continuous.

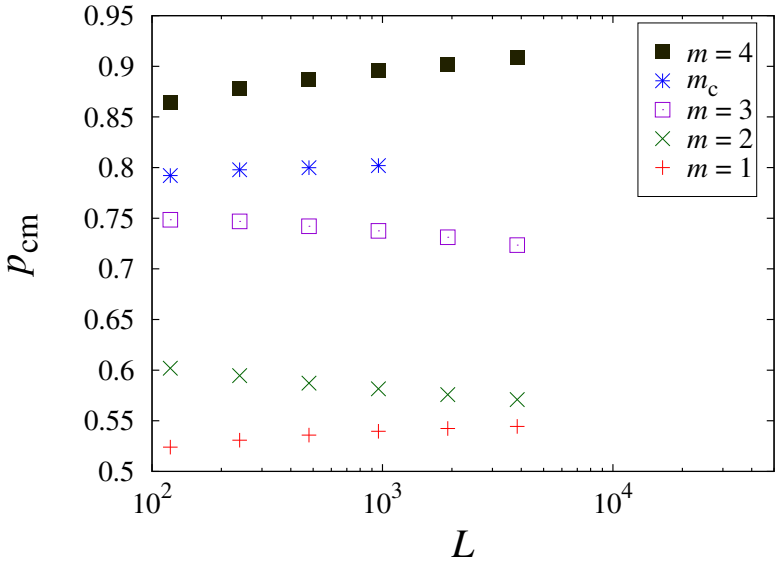

Fig. 2.16: Percolation threshold p_{cm} is plotted against linear size L for 2D partially directed lattice. Each data point represents simulation results averaged over 10^4 samples. Above $m_c \approx 3.3$ the thresholds converge to $p_c(\infty) = 0.55$, while below m_c they converge to unity. This indicates that the threshold at $m = m_c$ defines a horizontal line below and above which the percolation phase transition is continuous and discontinuous, respectively.

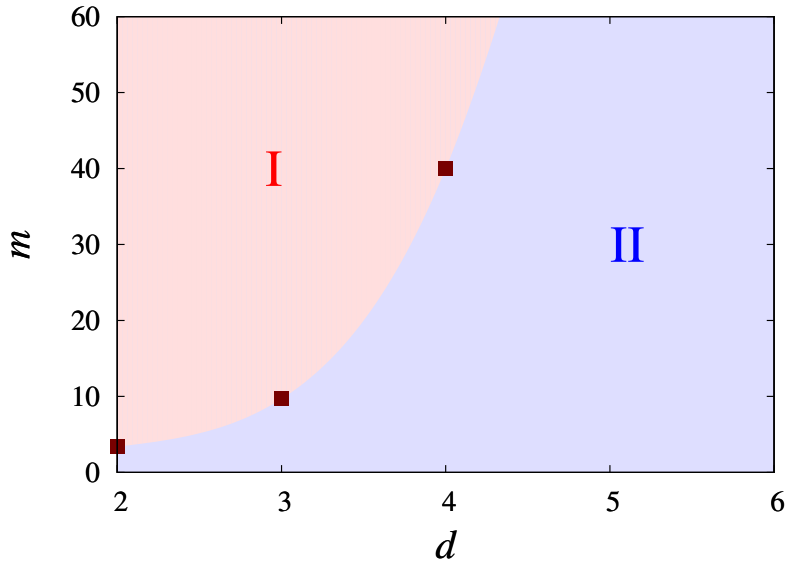

Fig. 2.17: The critical number of candidates m_c plotted for each dimension. m_c diverges to infinity at the upper critical dimension $d_c = 5$ and is not shown in the plot. The phase transition is discontinuous above the curve connecting these points and continuous below it. Since $m_c(d_c = 5) = \infty$, one cannot observe discontinuous phase transition in $d \geq 5$.

line between these two regimes. The inset in Fig. 2.15 shows that $\varphi = d - d_{BB}$ drops to 0 at the upper critical dimension $d_c = 5$ of directed percolation. As is the case in bidirectional lattice, we have diverging m_c above d_c and therefore the system only exhibits second-order transition in this region. Fig. 2.17 illustrates this point. $m_c(d = 4)$ has a high but still finite value, but past $d = 5$ no first-order transition can be observed for any values of m. Roman numerals are used to indicate of what order the phase transition in the region is.

The values obtained thus far for d_{BB} and m_c in dimensions up to $d = 6$ are listed in TABLE 2.1.

Table. 2.1: The values for fractal dimensions of bridge bonds and the critical number of candidates obtained by simulations are listed for various dimensions.

	DS		Tilted		PDS	
d	d_{BB}	m_c	d_{BB}	m_c	d_{BB}	m_c
2	1.072	2.155	1.38	3.23	1.41	3.39
3	2.10	3.33	2.60	7.50	2.69	9.68
4	3.16	4.76	3.72	14.29	3.9	40.0
5	4.25	6.66	4.67	15.15	5.0	∞
6	5.34	9.09	5.5	12.0	6.0	∞

Chapter 3

Roughness Exponent

If a directed square lattice is grown to $p \to 1$ while prohibiting the occupation of bridge bonds, one could observe an inclined boundary emerging between the two connected clusters. One example of this surface is illustrated in Fig. 3.18, which shows the boundary formed between the two colored clusters. The shape of this boundary, however, is exotic, since the directed bonds allow the formulation of tilted penninsulas.

A revised boundary can be formed by viewing the bottom cluster as liquid, thereby ignoring any top-connected cluster that comes below it on the account that the liquid will wet all cells beneath it. Note that this treatment is very similar to the rules of surface growth used in DPD models. Fig. 3.18 marks the revised boundary with a dotted black line, and the preferred inclination is shown as solid red line. x_i is the deviation of the dotted surface from the red line, and h_i is the horizontal gap between the two. We wish to calculate the standard deviation of x_i,

$$\sigma_x^2 = \frac{1}{L}\sum_i x_i^2 - \left(\frac{1}{L}\sum_i x_i\right)^2, \tag{3.1}$$

so that

$$\sigma_x \sim L^{\alpha} \tag{3.2}$$

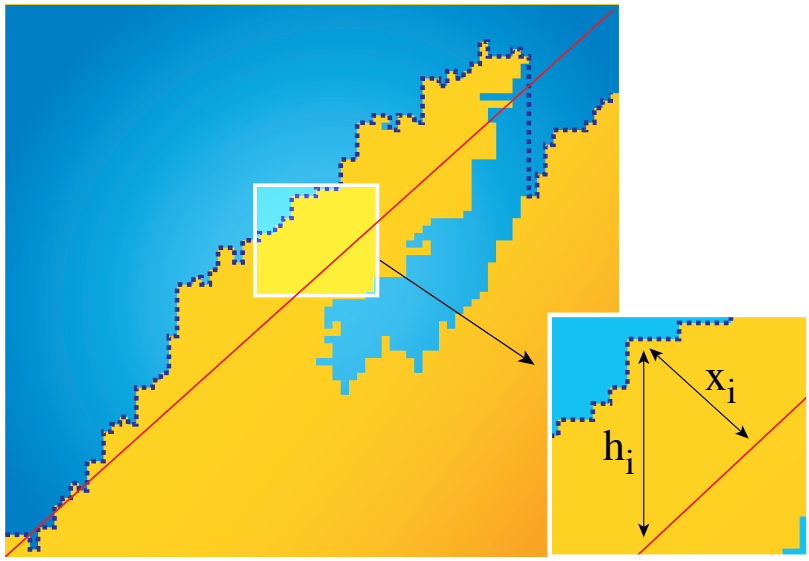

Fig. 3.18: A sample 70×70 directed 2D lattice grown to $p = 1$ exluding bridge bonds. The red and blue areas represent nodes connected to the top and bottom surfaces. We define a surface similar to that created by the DPD model, thus we sample out the maximum height of the boundary for each horizontal unit length. This new surface is plotted with dotted black line. The distance from this surface to red line x_i must be measured, but instead we measure h_i, since it only differs from x_i by a constant factor and does not affect the roughness exponent.

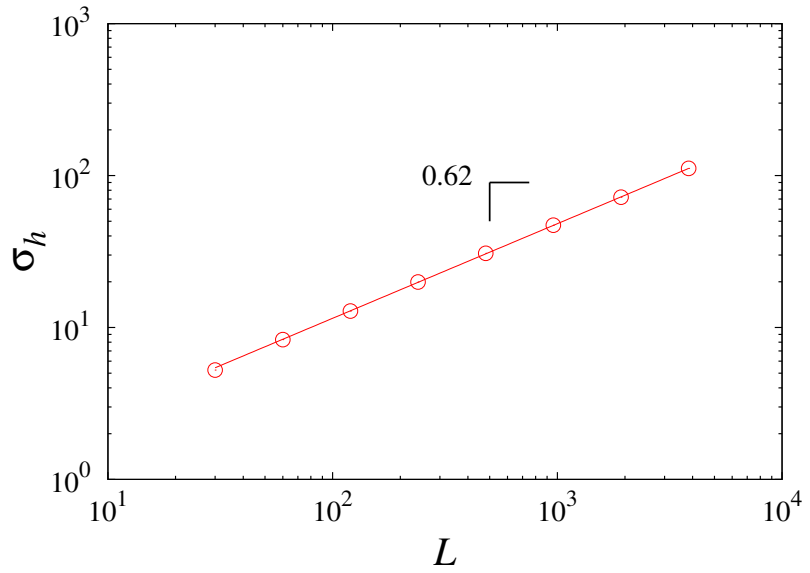

Fig. 3.19: The standard deviation of height σ_h is plotted against linear size L for 2D directional lattice at $p = 1$. Data points represent simulation results averaged over 10^4 samples, and solid line mark the best fit. The roughness exponent of 2D turns out to be 0.62, which is similar to the roughness exponent 0.63 of 2D DPD models.

can be used to measure the roughness exponent α. However, this calculation can be simplified by observing that the standard deviation of h_i, σ_h, is in fact a constant factor times σ_x:

$$\sigma_h^2 = \frac{1}{L}\sum_i h_i^2 - \left(\frac{1}{L}\sum_i h_i\right)^2 \tag{3.3}$$

$$= \frac{1}{L}\sum_i \frac{x_i^2}{\cos^2\theta} - \left(\frac{1}{L}\sum_i \frac{x_i}{\cos\theta}\right)^2 \tag{3.4}$$

$$= \frac{1}{\cos^2\theta}\sigma_x^2 \tag{3.5}$$

where θ is the inclination (45° in 2D), and $h_i \cos\theta = x_i$ has been used.

Fig. 3.19 plots the standard deviation of h_i against the linear system size

L for 2D. The data points clearly follow power law with exponent $\alpha(2\mathrm{D}) = 0.62$, which is similar to, but lower than, the roughness exponent $\alpha = 0.63$ of DPD models.

Chapter 4

Conclusion

We have extended the concepts of bridge bonds and fractal dimensions used in ordinary percolation models to various models of directed percolation. Probabilistic and numerical analysis suggest that the bridge bonds follow power law similar to ordinary percolation, and that the critical exponent ν should in this case be replaced by its analog of principal direction of percolation, $\nu_{||}$. Simulation results show that fractal dimensions of directed percolation are highly sensitive to the boundaries of the system as well as the structure of the lattice. Numerial data also confirms the validity of relation between fractal dimensions of bridge bonds and the continuity of percolation phase transition in the spanning-cluster-avoiding model, which was shown to hold in ordinary percolation [13]. The scaling behavior of cutting bonds have been investigated in relation to that of bridge bonds.

Moreover, we defined a surface that can be constructed from the bridge bonds of directed percolation. Taking into account the tendency to be inclined, the fluctuation of the surface has been measured which was in turn used to calculate the roughness exponent. The obtained exponent in $2D$ is $\alpha \approx 0.62$, which is similar to $\alpha \approx 0.63$ of the QKPZ universality class. This seems to be due to the similar nature of this surface to one grown in the DPD model, with differences in the minor details of how to proceed after wetting a depinned cell.

There are certainly areas where further work is anticipated. It has been shown that fractal dimensions of bridge bonds are highly sensitive to the boundary conditions of the lattice, but how they are related is still an intriguing question that needs to be answered. Measurements of the critical exponents of N_{BB} differed by a notable value at the critical point, its value depending on the method used to calculate it, which means the methods are measuring different quantities. More work must be done to establish precisely what this difference is. Also, since we have obtained the roughness exponent in $2D$ directed percolation, one direction of future work can be the construction and definition of surfaces at higher dimensions. This can lead to the calculation of the roughness exponent in higher dimensions, thereby making a connection between the surface and some other universality class.

The bridge bonds in directed percolation opens up an interesting direction of research connecting the fractal dimensions, lattice structures, phase transitions, and surface roughness. We believe our work can serve as another step towards understanding the fundamental physics lying underneaths these concepts.

Bibliography

[1] E. Domany and W. Kinzel, Phys. Rev. Lett. **53**, 311 (1984).

[2] Y. Pomeau, Physica D **23**, 3 (1986).

[3] H. Chaté and P. Manneville, Physica D **32**, 409 (1988).

[4] J. Rolf, T. Bohr, and M. Jensen, Phys. Rev. E , R2503 (1998).

[5] J. M. López and H. J. Jensen, Phys. Rev. Lett. **81**, 1734 (1998).

[6] L.-H. Tang and H. Leschhorn, Phys. Rev. A **45**, R8309 (1992).

[7] S. V. Buldyrev, A.-L. Barabási, F. Caserta, S. Havlin, H. E. Stanley, and T. Vicsek, Phys. Rev. A **45**, R8313 (1992).

[8] M. Kardar, G. Parisi, and Y.-C. Zhang, Phys. Rev. Lett. **56**, 889 (1986).

[9] L.-H. Tang, M. Kardar, and D. Dhar, Phys. Rev. Lett. **74**, 920 (1995).

[10] A. Dıaz-Sánchez, L. Braunstein, and R. Buceta, Eur. Phys. J. B **21**, 289 (2001).

[11] E. Fehr, K. J. Schrenk, N. A. M. Araújo, D. Kadau, P. Grassberger, J. S. Andrade, and H. J. Herrmann, Phys. Rev. E **86**, 011117 (2012).

[12] K. Schrenk, N. Araújo, J. Andrade Jr, and H. Herrmann, Sci. Rep. **2** (2012).

[13] Y. S. Cho, S. Hwang, H. J. Herrmann, and B. Kahng, Science **339**, 1185 (2013).

[14] I. Jensen, Phys. Rev. Lett. **77**, 4988 (1996).

[15] I. Jensen, J. Phys. A **32**, 5233 (1999).

초 록

본드 스미기 모형은 특정한 방향 선호도가 없는 유클리드 공간에서 본드를 임의의 순서대로 연결해 나갈 때 서로 반대편의 끝을 잇는 거대 송이의 생성을 탐구하기 위한 수학적인 모형이다. 본드는 크게 연결본드와 비연결본드로 나뉘는데, 여기서 연결본드란 연결되는 순간 여과경로를 생성하는 본드를 말한다. 이러한 연결본드의 연결을 억제한 상태로 본드를 채워나가다 보면 마지막에는 시스템이 두 개의 덩어리로 나뉘게 되고, 이 연결본드들은 쪽거리 구조를 가지게 된다. 최근 연구로 이 집합의 쪽거리 차원이 폭발적 여과 상전이의 연속성과 밀접한 관련성을 갖다는 것이 밝혀졌다. 하지만, 본드들이 방향성을 가지는 격자구조에서는 이러한 연결본드에 대해 알려진 것이 거의 없는 상황이다. 이 논문에서 우리는 방향성을 갖는 격자구조에서 연결본드가 역시 쪽거리 구조를 가진다는 점을 확인하고, 이 구조의 쪽거리 차원을 여러 차원에서 계산한 후 등방성 격자에서의 값과 비교해보고자 한다. 또한, 이러한 쪽거리 차원들이 여과 상전이의 연속성과 어떠한 관련이 있는지 탐구하고, 이러한 결과들이 갖는 파급효과에 대해 논해보도록 하겠다.

주요어 : 여과 상전이, 방향성 스미기, 다리본드, 불연속 여과 상전이, 쪽거리 차원

학번 : 2011-20426